Article

pubs.acs.org/Biomac

Ratiometric Fluorescent Biosensor for Hyaluronidase with Hyaluronan As Both Nanoparticle Scaffold and Substrate for Enzymatic Reaction

Huafei Xie, Fang Zeng,* and Shuizhu Wu*

College of Materials Science & Engineering, State Key Laboratory of Luminescent Materials & Devices, South China University of Technology, Guangzhou 510640, China

Supporting Information

ABSTRACT: Hyaluronidases (HAase) are involved in various physiological and pathological processes and have been reported as urinary marker for bladder cancer. In this study, a novel ratiometric fluorescent sensing system based on both aggregation-induced emission (AIE) and aggregation-induced quenching (ACQ) was developed to quantitatively assess hyaluronidase level. First, a tetraphenylethylene derivative with positive charges (TPE-2N$^+$, typical AIE molecule) at both ends and an anthracene derivative with positive charge at one end (AN-N$^+$, typical ACQ molecule) was synthesized. These two positively charged compounds were then mixed with a negatively charged hyaluronan (HA), which induced the aggregation of the compounds as well as the nanoparticles formation as a result of electrostatic complexation, with TPE-2N$^+$ acting as cross-linking agent. The aggregation also caused the efficient quenching of the emission of AN-N$^+$ due to ACQ effect, as well as the fluorescence enhancement of TPE-2N$^+$ due to AIE effect. In the presence of HAase, the enzymatic reaction led to the degradation of HA and triggered disassembly of the nanoparticles; as a result, the emission of AN-N$^+$ was restored and that of TPE-2N$^+$ was suppressed. This fluorescence variation affords the system a robust ratiometric biosensor for HAase, and the ratio of fluorescence intensity for AN-N$^+$ (I_{414}) to that for TPE-2N$^+$ (I_{474}) can be used as the sensing signal for detecting HAase activity. In this system, hyaluronan serves not only as the scaffold for nanoparticle formation but also as the substrate for enzymatic reaction. This assay system is operable in aqueous media with very low detection limit of 0.0017 U/mL and is capable of detecting HAase in biological fluids such as serum and urine. This strategy may provide a new and effective approach for developing other enzyme assays.

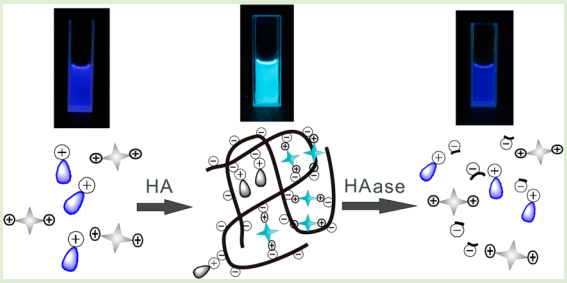

1. INTRODUCTION

Hyaluronan (hyaluronic acid, HA) is a linear mucopolysaccharide, which is highly negatively charged and can be found in the extracellular matrix of all vertebrates and in the capsule of some bacteria.[1−3] Hyaluronidases are the extracellular matrix-digesting endoglycosidases that predominately degrade high-molecular-weight hyaluronan into fragments with low molecular weights.[4,5] Hyaluronidases are involved in a variety of physiological and pathological processes, such as fertilization, embryogenesis, maintenance of the elastoviscosity of liquid connective tissues including joint synovial and eye vitreous fluid, control of tissue hydration and water transport, wound healing, inflammation, and tumor growth.[6−10] Bladder cancer is among the five most common malignant tumors, it is also the second most common tumor of the genitourinary tract and the second most common cause of death in patients with genitourinary cancers.[11,12] Recently, HAase has been reported as urinary marker for bladder cancer, and urinary HAase level has been employed as an assessment in early diagnosis of bladder cancer.[4,5] Due to its physiological importance, sensitive and selective method to detect HAase level is of great significance.

Currently, a number of methods, such as physicochemical methods, chromatographic methods, and colorimetric approaches[13−17] have been used to measure HAase level. However, most of these methods require time-consuming preparation steps. While fluorescence technique offers distinct advantages including, ease of use, high sensitivity, and the real-time monitoring capability and usability in biological samples.[18−22] The reported fluorescent methods for detecting HAase usually require substrate modification, for example, modifications at the free carboxyl groups of HA substrate with fluorescein or biotin, which could affect the activity of HAase.[23] In addition, these fluorescent methods employ single fluorescent intensity as the sensing signal; hence, the sensing may well be interfered by a variety of factors including variations in excitation intensity, emission collection efficiency, and probe concentration.[24−28] In comparison, ratiometric fluorescent probes that adopt simultaneous recording of two fluorescence intensity signals in the presence and absence of

Received: June 17, 2014
Revised: July 22, 2014
Published: July 28, 2014

dx.doi.org/10.1021/bm500890d | Biomacromolecules 2014, 15, 3383−3389

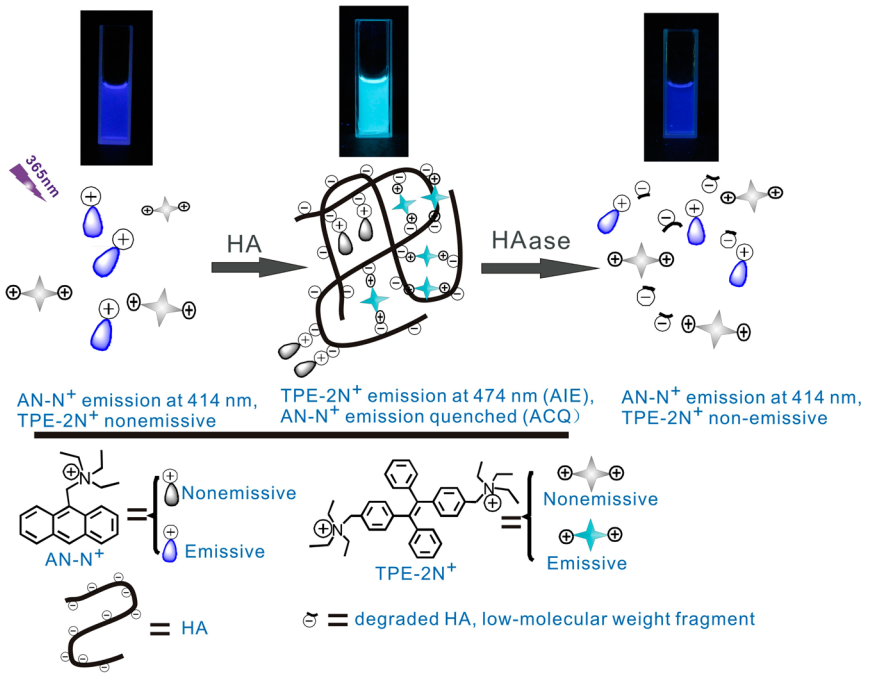

Figure 1. Schematic illustration for the assay system and its ratiometric fluorescent response to HAase.

analyte can minimize some interfering factors and allow for more accurate detection.[29−31] Therefore, for HAase detection, there is still a high demand to improve the available probes for utilization in biological samples with respect to their convenience, sensitivity, ratiometric sensing, and unmodified HA substrate.

Ratiometric fluorescent sensing can be realized through various mechanisms such as fluorescence resonance energy transfer (FRET) and incorporation of a reference dye.[32,33] The preparation of these ratiometric fluorescent sensing systems usually requires relatively complicated synthetic process. For example, to prepare FRET-based ratiometric fluorescent sensing, usually two fluorophores need to be incorporated simultaneously into the sensing system, which increases synthetic complexity.[34,35] For most of the ratiometric fluorescent sensors, a variety of common fluorophores were used as the emissive units.[36,37] These fluorophores usually display aggregation-caused quenching (ACQ) in aqueous or physiological media, and this is attributed to the nonradiative relaxation of the aggregates' excited states.[38−40] Contrary to conventional fluorophores, some organic compounds are nonemissive in molecularly dissolved state but become highly emissive when aggregated due to the restricted intramolecular rotation. This unusual emission phenomenon was referred to as "aggregation-induced emission" (AIE).[41−44]

In this study, we sought to design a ratiometric sensing system for HAase with unmodified substrate. By employing unmodified HA as both the nanoparticle formation scaffold and the substrate for enzymatic reaction, and making use of both the ACQ effect and AIE effect, we fabricated a new ratiometric biosensor for HAase. The schematic illustration for the ratiometric fluorescent detection is shown in Figure 1. First, a tetraphenylethylene derivative with positive charges at both ends (TPE-2N$^+$, typical AIE molecule) and an anthracene derivative with positive charge at one end (AN-N$^+$, typical ACQ molecule) were synthesized, then these two positively charged compounds were mixed with the negatively charged hyaluronan (HA), and nanoparticles readily formed due to electrostatic complexation, with TPE-2N$^+$ acting as cross-linking agent. Because of the aggregation, the emission of AN-N$^+$ was efficiently quenched due to ACQ effect, while the emission of TPE-2N$^+$ was greatly enhanced due to AIE effect. In the presence of HAase, the enzymatic reaction led to the degradation of HA, which in turn triggered the nanoparticle disassembly; as a result, the emission of AN-N$^+$ was restored and that of TPE-2N$^+$ was suppressed. The ratio of fluorescence intensity for AN-N$^+$ to that for TPE-2N$^+$ can therefore be used as the sensing signal for detecting HAase activity. Compared with other HAase assays, this approach shows comparable or even better sensing performance with no need for substrate modifications (which may affect the activity of enzyme). Additionally, due to the ratiometric sensing mechanism, fluorescence color change during the detection process can be easily observed by naked eyes under a hand-held UV lamp. This assay herein was also investigated for detection of HAase activity in biological fluid such as human serum and urine.

2. EXPERIMENTAL SECTION

2.1. Materials and Reagents. Hyaluronan (molecular weight: 1000 kDa) from bovine vitreous humor, 9-(chloromethyl)anthracene, titanium tetrachloride, potassium tetraborate, p-dimethylaminobezaldehdye, 4-methylbenzophenone, and bovine testicular hyaluronidase (EC 3.2.1.35, type 1-S, 476 U/mg) were purchased from Sigma-Aldrich, and used as received. Azobis(isobutyronitrile) (AIBN), N-bromobutanimide (NBS), dimethyl sulfoxide (DMSO for HPLC), *N*,*N*-dimethylformamide (DMF) and triethylamine (TEA) were obtained from Alfa Aesar. Sodium chloride, dichloromethane, CCl_4, tetrahydrofuran (THF), acetone, diethyl ether, petroleum ether, and other inorganic salts were analytically pure reagents. The water used in this study was the triple-distilled water which was further treated by ion exchange columns and then by a Milli-Q water purification system.

2.2. Synthesis of (9-Triethylammonium) Anthracene Chloride (AN-N$^+$). The synthesis was briefly described as follows: into a 100 mL round-bottom flask fitted with a condenser were added the 9-(chloromethyl)anthracene (226.7 mg, 1 mmol) and 20 mL of acetone, and then triethylamine (303.57 mg, 3 mmol) was added. The mixture

dx.doi.org/10.1021/bm500890d | *Biomacromolecules* 2014, 15, 3383−3389

was refluxed at 60 °C for 8 h. The precipitate was filtrated and washed by ethyl ether (3 × 20 mL). After being dried in vacuum oven, the solid was obtained in 51.6% yield. ^{1}H NMR (400 MHz, D_2O), δ (TMS, ppm): 8.05−7.96 (s, 1H), 7.83−7.75 (d, 2H), 7.72−7.63 (d, 2H), 7.54−7.43 (t, 2H), 7.41−7.33(t, 2H), 4.49−4.58 (s, 2H), 3.12−2.93 (m, 6H), 0.82−0.64 (t, 9H). MS (ESI): m/z 291.1 $[M]^+$.

2.3. Synthesis of 1,2-bis(4-Methylphenyl)-1,2-diphenylethene (Compound 2). This compound was prepared according to previously published experimental procedures.[45] The synthesis was briefly described as follows: Into a vacuum-evacuated, nitrogen-filled 250 mL two-necked, round-bottomed flask was added 3.92 g (0.02 mol) of 4-methylbenzophenone and 100 mL of THF. The solution was cooled down to −5 °C, into which $TiCl_4$ (5.69 g, 0.03 mol) and Zn dust (2.62 g, 0.04 mol) were added. After being refluxed overnight, the reaction mixture was cooled to room temperature and filtered through a pad of silica gel. The filtrate was concentrated and the crude product was further purified by a silica gel column using petroleum ether as eluent. A white solid was obtained in 85.2% yield (3.06 g). ^{1}H NMR (400 MHz, DMSO-d_6), δ (TMS, ppm): 7.15−7.07 (m, 4H), 6.98−6.91 (m, 10H), 6.86−6.82 (m, 4H), 2.21 (d, J = 5.6, 6H). MS (ESI): m/z 360.4 $[M]^+$.

2.4. Synthesis of 1,2-bis[4-(Triethylammoniomethyl)-phenyl]-1,2-diphenylethene Dibromide (TPE-2N$^+$). This TPE-2N$^+$ was prepared according to previously published experimental procedures.[46] The synthesis was briefly described as follows: Into a 25 mL round-bottom flask was added 0.36 g (1 mmol) of **2**, 0.356 g (2 mmol) of freshly recrystallized NBS, and a catalytic amount of AIBN in 10 mL of CCl_4. The solution was refluxed at 80 °C for 10 h. After being cooled to room temperature, the solution was filtered and the filtrate was concentrated. The solvent was removed by vacuum-rotary evaporation procedure and the crude product was obtained. Afterward, into a 50 mL round-bottom flask fitted with a condenser were added the crude product **3** (512 mg, 1 mmol) and 20 mL of acetone, and then, triethylamine (607.14 mg, 6 mmol) was added. The mixture was refluxed at 60 °C for 8 h. The precipitates was filtrated and washed by acetone (3 × 20 mL). After being dried in vacuum oven, the white solid was obtained in 25.6% yield. ^{1}H NMR (400 MHz, DMSO-d_6), δ (TMS, ppm): 7.34−7.31 (m, 4H), 7.19−7.10 (m, 10H), 7.03−7.00 (m, 4H), 4.44−4.41 (s, 4H), 3.10−3.20 (m, 12H), 1.30−1.20 (m, 18H). MS (ESI): m/z 280.1 $[M\text{-}2Br]^{2+}$.

2.5. Measurements. ^{1}H NMR spectra were recorded on a Bruker Avance 400 MHz NMR Spectrometer. Mass spectra were obtained through Bruker Esquire HCT Plus mass spectrometer. Fluorescence spectra were recorded on a Hitachi F-4600 fluorescence spectrophotometer with excitation wavelength being 365 nm. The particle size and distribution was determined by dynamic light scattering (DLS) on a Malvern Nano-ZS90 particle size analyzer at a fixed angle of 90° at 25 °C. Transmission electronic microscopy (TEM) experiments were carried out by mounting an aqueous drop (∼15 μL) of the solution onto a carbon-coated copper grid and observation was carried out on a JEM-2010HR transmission electron microscopy (Japan).

2.6. Preparation of the Sensing System'S Stock Solution. The sensing system's stock solution was prepared by dissolving AN-N$^+$ and TPE-2N$^+$ and HA in buffer under stirring, and nanoaggregates readily formed due to one-pot assembly through electrostatic complexation between AN-N$^+$ and TPE-2N$^+$ and HA in buffer. Briefly, HA was dissolved in PBS buffer (pH 4.3, 0.1 mM), and AN-N$^+$ and TPE-2N$^+$ solutions (with different molar ratios) were simultaneously added under stirring for 2 min. Then, the nanoparticle dispersions were obtained and stored at 2−8 °C for use.

2.7. Enzyme Triggered Disassembly Process. The HAase detection experiments were conducted as follows: 0.5 mL HAase solution of varying concentrations was added to 2.5 mL of the sensing system solution (nanoparticle dispersion) and the mixtures (in the final testing solution, 4 μM AN-N$^+$/26 μM TPE-2N$^+$/0.003 mg/mL HA were kept constant) were incubated at 37 °C for a certain period of time. Termination of enzymatic reaction was achieved by heating the mixtures in boiling water for 10 min. After cooling the mixtures to room temperature, the fluorescence spectrum was recorded with the excitation at 365 nm and the ratios of fluorescence intensity at 414 and 474 nm (I_{414}/ I_{474}) were calculated.

2.8. HAase Activity Detection in Biological Fluid Samples. The urine was obtained from healthy adult men and serum was obtained from a local hospital. For HAase detection in serum samples, the fluorescence measurements were recorded for samples containing the sensing system solution (final concentration: AN-N$^+$ 4 μM/TPE-2N$^+$ 26 μM/HA 0.003 mg/mL) with or without HAase in PBS buffer (pH 4.3, 0.1 mM) at 37 °C (for the samples with added HAase, the measurements were conducted after 100 min of mixing), and the fluorescence intensity ratios I_{414}/I_{474} were calculated. The final concentration of the serum in the test solutions is 50-fold diluted.

The determination of HAase level in human urine samples was performed as follows: First, the urine samples were buffered at pH 4.3 using NaH_2PO_4, Na_2HPO_4, and NaCl. Then, 100 μL of each urine sample was mixed properly with 20 mg of chitosan and then centrifuged at 8000 rpm for 10 min (chitosan is insoluble in urine sample and was used to agglomerate all negatively charged moieties present in urine sample without adsorbing HAase molecules, in accordance with literature report).[16] Then, urine supernatant was added into the probe solution, the fluorescence measurements were conducted as mentioned previously.

3. RESULTS AND DISCUSSION

3.1. Preparation and Characterization of the Assay System. To prepare the assay system, its two fluorophore components, TPE-2N$^+$ and AN-N$^+$, were first synthesized, respectively; the synthesis routes for the two fluorohpores were described in Supporting Information (SI) Scheme S1. The final products were characterized by ^{1}H nuclear magnetic resonance (^{1}H NMR) and mass spectrometry (MS) (SI Figures S1−S4), which confirmed the successful synthesis of TPE-2N$^+$ and AN-N$^+$.

Due to the existence of quaternary ammonium group, AN-N$^+$ is well soluble in PBS buffer solution (0.1 mM, pH 4.3; previous studies have shown that the optimal pH for HAase is around 4.3[13,16,51]) and shows blue emission at around 414 nm. Upon gradual addition of HA, the fluorescence intensity of AN-N$^+$ at around 414 nm decreases accordingly (SI Figure S5). This is simply because, AN-N$^+$ molecules will bind and/or aggregate along the HA chain due to electrostatic complexation between HA and AN-N$^+$, and also the ACQ effect of AN-N$^+$; hence, as the amount of HA is increased, the aggregation is enhanced, corresponding the fluorescence of AN-N$^+$ further weakens. On the contrary, the fluorescence intensity of TPE-2N$^+$ in PBS buffer solution is very weak due to the lack of aggregation and the AIE-active feature of this fluorophore; however, the emission of the fluorophore solution at 474 nm is greatly enhanced upon addition of HA as shown in SI Figures S6 and S7 (the absorption spectra are shown in SI Figure S8). The electrostatic interactions between the positively charged TPE-2N$^+$ and the negatively charged HA results in the formation of nanoaggregates, and the fluorescence intensity increases significantly due to the AIE effect.

In principle, the HA/AN-N$^+$ or HA/TPE-2N$^+$ system may be used to detect HAase activity; as shown in SI Figures S5 and S6, it is clear that the system consisting of only one probe (either AN-N$^+$ or TPE-2N$^+$) and HA can also function as the detection system for HAase; however, these two systems can only function either as the Turn-ON or Turn-OFF sensors for HAase. While ratiometric fluorescent sensing method depends on simultaneous variation of fluorescence intensities at two different wavelengths, thus providing a built-in self-calibration and higher accuracy for quantitative analysis.[47]

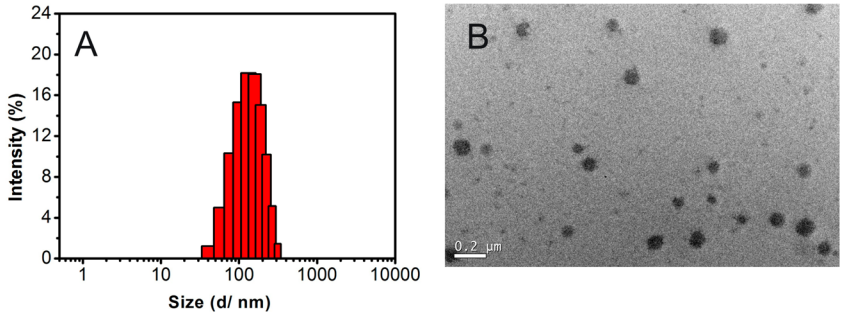

Figure 2. (A) Size distribution of the sensing system in PBS buffer solution (pH 4.3) (4 μM AN-N$^+$/26 μM TPE-2N$^+$/0.003 mg/mL HA) determined by DLS; (B) TEM image of the sensing system.

3.2. Fluorescent Response of the Sensing System toward HAase. To investigate the biosensor's fluorescent response toward HAase, we measured the fluorescent spectra of the sensing system in the absence or presence the different concentrations of HAase. The fluorescence spectra of the system were periodically recorded during incubation of the assay system with HAase at 37 °C in PBS buffer (0.1 mM, pH 4.3).

To determine the suitable AN-N$^+$/TPE-2N$^+$ ratio for preparing the sensing system, we first measured the fluorescence spectra of the ensemble with different molar ratios by keeping the concentration of HA constant at 0.003 mg/mL and the amount of HAase at 15 U/mL (SI Figures S9). When the AN-N$^+$/TPE-2N$^+$ ratio is in the range 4:26−7:20, the fluorescence intensities of two fluorophores in the presence or absence of HAase are comparable, and in the following HAase detection experiments, we adopted the ratio of 4:26. It is clear, as the enzymatic reaction time is increased, the fluorescence intensity at 474 nm decreased gradually simultaneously with a gradual increase of emission at 414 nm; and there exists a clear isosbestic point.

The photobleaching of the sensing system in PBS buffer was also investigated. Despite direct exposure to UV lamps (254 and 365 nm simultaneously) for 0 to 180 min, the fluorescence spectra and the emission intensity ratio I_{414}/I_{474} of the sensing system show only slight change (SI Figure S10), this indicates that the nanoaggregates formed by AN-N$^+$/TPE-2N$^+$/HA are stable and have very good photostability. Moreover, we studied the nanoaggregates using DLS and TEM. The formation of spherical nanoaggregates with a diameter in the range 80−100 nm has been observed by TEM, as shown in Figure 2, this size is smaller than that (~170 nm) determined by the DLS.

The kinetic activity of the enzymatic reaction was determined by measuring the time-dependent fluorescence changes of the sensing system (4 μM AN-N$^+$/26 μM TPE-2N$^+$/0.003 mg/mL HA) in the presence of different concentrations of HAase, as shown in Figure 3 and Figure 4. In the absence of HAase, we did not notice any changes in the fluorescence spectrum, which also proves the stability of the system. The time-course experiments show that the emission intensity ratio of I_{414}/I_{474} gradually increases as enzyme concentration and time increase, and reaches a plateau after 85 min of reaction time when HAase level is kept at 10 U/mL. To ensure complete reaction, the incubation time of 100 min was employed in all other experiments. Fluorescence color change of the sensing system in the absence of HAases and in the presence of different HAase levels can be clearly observed form blue to greenish blue under a hand-held UV lamp (SI Figure S11).

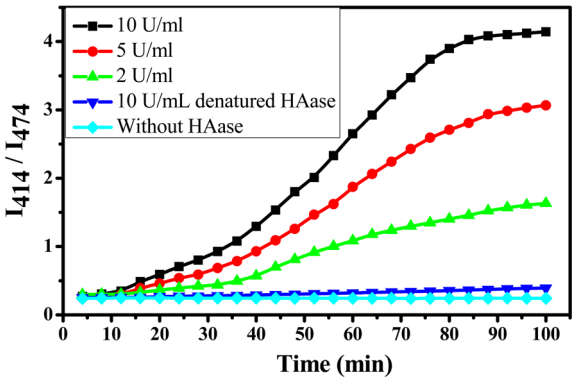

Figure 3. Plot of the fluorescence intensity I_{414}/I_{474} of the sensing system (4 μM AN-N$^+$/26 μM TPE-2N$^+$/0.003 mg/mL HA) versus reaction time in the presence of different amounts of HAase and the denatured enzyme in PBS buffer solution (pH 4.3) (λ_{ex} = 365 nm).

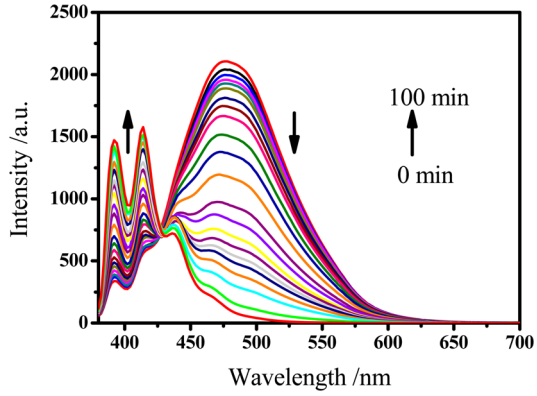

Figure 4. Time course of fluorescence spectra of the sensing system (4 μM AN-N$^+$/26 μM TPE-2N$^+$/0.003 mg/mL HA) in the presence of HAase. The measurements were conducted with HAase (15 U/mL) in PBS buffer solution (pH 4.3, 0.1 m). Spectra measured every 5 min are displayed (λ_{ex} = 365 nm).

3.3. Detection Limit of the Biosensor. To demonstrate the efficiency of this sensing system in the measurement of HAase, various HAase levels (0.005−10 U/mL) were added to the sensing system solutions (4 μM AN-N$^+$/26 μM TPE-2N$^+$/0.003 mg/mL HA), and then, the fluorescent spectra were measured after 100 min incubation. As shown in Figure 5, the fluorescent intensities at 414 nm increase, while those at 474 nm decrease with increasing levels of HAase. The fluorescence intensity ratio of I_{414}/I_{474} were linearly related to the HAase level at the low concentration range of 0.005−0.2 U/mL (2.38−95.2 mg/mL; SI Figure S12). The detection limit was

dx.doi.org/10.1021/bm500890d | Biomacromolecules 2014, 15, 3383−3389

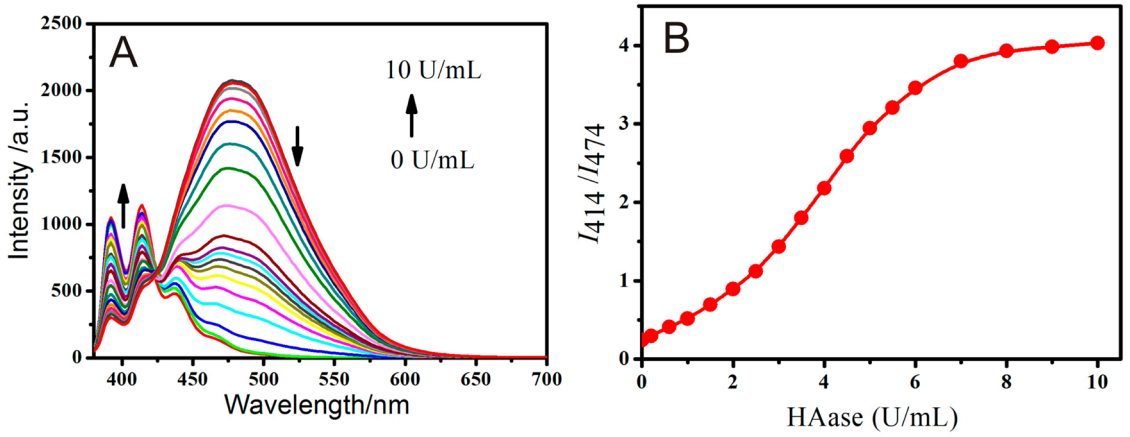

Figure 5. (A) Fluorescence spectra of the sensing system (4 μM AN-N$^+$/26 μM TPE-2N$^+$/0.003 mg/mL HA) in the absence of HAase and in the presence of different HAase levels in PBS buffer solution (0.1 mM, pH 4.3). (B) Fluorescence intensity ratio of I_{414}/I_{474} for the sensing system (4 μM AN-N$^+$/26 μM TPE-2N$^+$/0.003 mg/mL HA) in PBS buffer solution (0.1 mM, pH 4.3) as a function of HAase level (λ_{ex} = 365 nm).

determined to be as low as 0.0017 U/mL (0.81 mg/mL). These results show that this sensing system is sensitive to hyaluronidase activity. Since HAase level in normal human serum is 0.256 ± 0.198 U/mL, and HAase level in normal human urine is 0.0042 ± 0.0012 U/mL,[48] with the detection limit of 0.0017 U/mL, this system has the potential to be used for HAase level determination in biological fluids samples.

The sensing mechanism involves nanoparticle formation between the two positively charged fluorophores (the AIE-active TPE-2N$^+$ and the ACQ-active AN-N$^+$) and the negatively charged HA, as well as the nanoaggregate disassembly triggered by enzymatic reaction of HAase. To further confirm the sensing mechanism, we studied the nanoaggregate formation and disassembly triggered by enzymatic reaction by TEM and DLS measurements. As shown in Figures 6 and 7, in the absence of HAase, the size of

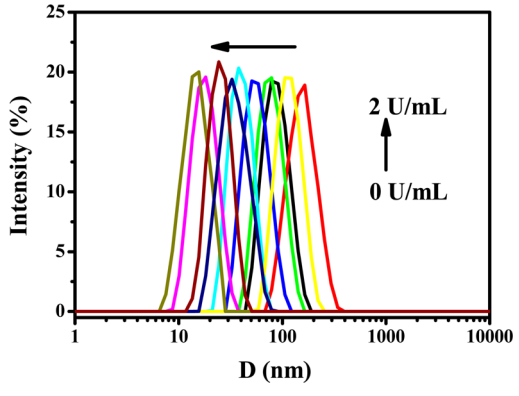

Figure 6. Size distribution of the nanoaggregates determined by dynamic light scattering (DLS) upon addition of different amounts of HAase.

the nanoparticles formed by the sensing system is around 170 nm by DLS and 80−100 nm by TEM. Upon addition of HAase, the enzymolysis leads to the degradation of HA and corresponding disassembly of the nanoparticles. With the increased HAase levels, the size of the nanoparticles decreases gradually. Similar results were also obtained by TEM (Figure 7). In the presence of HAase, HA is degraded into fragments with small molecular weights; hence, the electrostatic interactions between these negatively charged fragments and the positively charged TPE-2N$^+$ and AN-N$^+$ can no longer form nanoaggregates, and both fluorophores are water-soluble; as a result, the AIE effect of TPE-2N$^+$ and the ACQ effect of AN-N$^+$ are turned off. To further confirm that the nanoaggregate disassembly is triggered by the enzymatic reaction of HAase, we heated the nanoaggregate sensing system up to 100 °C without the addition of HAase and then measured the size of the nanoparticles by DLS, as shown in SI Figure S13. It can be seen that, without addition of HAase, the nanoaggregate size basically remains unchanged, which again proves the disassembly is caused by HAase.

3.4. HAase Detection in Biological Fluid Samples. Based on the above results, we set out to evaluate the efficacy of this assay system in real biological samples. It was reported that high urinary and serum levels of HAase have been used for detection of high-grade bladder carcinoma,[49,50] so we measured HAase levels in the urine and serum with different levels. In this study, the HAase level of each sample was determined from the standard curve (SI Figure S12) and listed in SI Table S1 and Table S2. For urine samples, chitosan, which is insoluble in urine sample, was used to agglomerate all negatively charged moieties present in urine sample without adsorbing HAase molecules (HAase has relatively low molecular weight), according to literature-reported method.[16] The endogenous (originally existing) HAase in urine and diluted serum sample was determined by the system and the traditional colorimetric Morgan−Elson assay method[51] for comparison. As can be seen from the results, the deviation between the two assay methods is less than 10%, and the endogenous HAase levels for the urine and undiluted serum sample are then calculated as 5.12 × 10^{-3} U/mL and 0.317 U/mL, respectively. In addition, the possible interference of biologically relevant species (including salts, vitamins, and amino acids) was also investigated, and the results are shown in SI Figure S14. It is obvious that only HAase induces a prominent fluorescence change, whereas the addition of other species under the same conditions leads to almost no fluorescence change. These results, in combination with the unique specificity of the enzymatic reaction, confirm that the system has good selectivity toward HAase over other biologically relevant species.

Furthermore, the sensing system has also been successfully used to detect the HAase levels in urine and diluted serum samples spiked with HAase in this study. The recovery of added

dx.doi.org/10.1021/bm500890d | Biomacromolecules 2014, 15, 3383−3389

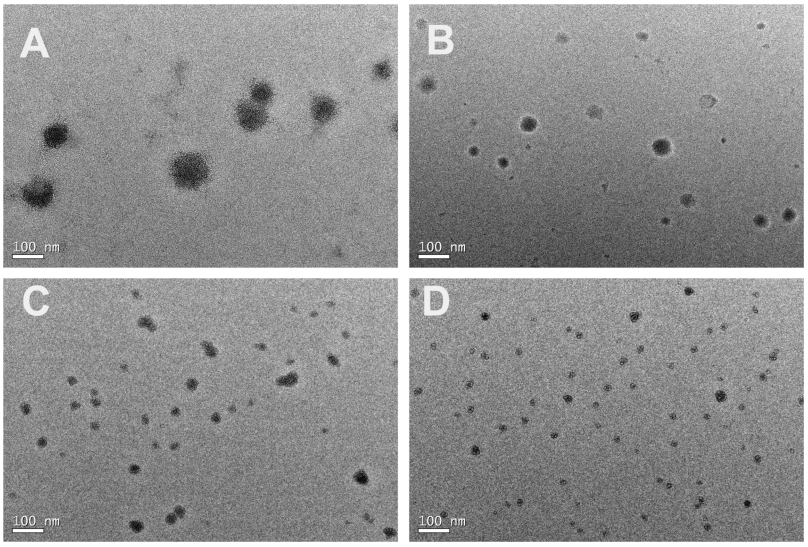

Figure 7. HR-TEM images of the assay systems with the addition of HAase (A, 0; B, 0.25; C, 0.5; D, 1.0 U/mL, respectively) placed on copper grids. Scale bar: 100 nm.

known amounts of HAase into the urine and serum samples are in the range 97.55−102.15% and 98.95−108.92%, these results suggest the accuracy and reliability of the present method for HAase determination, and this system could be used for diagnosis of bladder carcinoma. The sensing system's response toward HAase is repeatable and reproducible.

4. CONCLUSIONS

In summary, we successfully designed a fluorescent ratiometric biosensor for HAase through employing unmodified HA as the nanoparticle formation scaffold and the substrate for enzymatic reaction and by using the ACQ effect and AIE effect. Compared with other HAase assays, this approach shows comparable or better performance with no need for substrate modifications which may affect the activity of enzyme. Moreover, due to the ratiometric sensing mechanism, higher sensitivity and reliability can be achieved and the fluorescence color change during the detection process can be easily observed by naked eyes under a hand-held UV lamp. This assay herein can be used detection of HAase level in biological fluid such as human serum and urine. This strategy may offer a technically simple approach for designing ratiometric fluorescent sensing systems for detecting other biomolecules in biological samples.

■ ASSOCIATED CONTENT

Supporting Information

Synthetic routes, ^{1}H NMR spectra, mass spectra, fluorescence spectra, absorption spectra, photographs, determination of the detection limit, photobleaching experiment data, detection of HAase level in serum, and detection of HAase level in urine. This material is available free of charge via the Internet at http://pubs.acs.org.

■ AUTHOR INFORMATION

Corresponding Authors

*Tel.: +86-20-22236262. Fax: +86-20-22236363. Email: mcfzeng@scut.edu.cn.
*Email: shzhwu@scut.edu.cn.

Notes

The authors declare no competing financial interest.

■ ACKNOWLEDGMENTS

We gratefully acknowledge the financial support by the National Key Basic Research Program of China (Project No. 2013CB834702), and NSFC (21025415 and 21174040).

■ REFERENCES

(1) Kramer, M. W.; Escudero, D. O.; Lokeshwar, S. D.; Golshani, R.; Ekwenna, O. O.; Acosta, K.; Merseburger, A. S.; Soloway, M.; Lokeshwar, V. B. *Cancer* **2011**, *117*, 1197−1209.
(2) Lokeshwar, V. B.; Selzer, M. G. *Semin. Cancer Biol.* **2008**, *18*, 281−287.
(3) Veiseh, M.; Breadner, D.; Ma, J.; Akentieva, N.; Savani, R. C.; Harrison, R.; Mikilus, D.; Collis, L.; Gustafson, S.; Lee, T. Y.; Koropatnick, J.; Luyt, L. G.; Bissell, M. J.; Turley, E. A. *Biomacromolecules* **2012**, *13*, 12−22.
(4) Tan, J. X.; Wang, X. Y.; Li, H. Y.; Su, X. Y.; Wang, L.; Ran, L.; Zheng, K.; Ren, G. S. *Int. J. Cancer* **2011**, *128*, 1303−1315.
(5) Whatcott, C. J.; Han, H. Y.; Posner, R. G.; Hostetter, G.; Von Hoff, D. D. *Cancer Discovery* **2011**, *1*, 291−296.
(6) Chao, K. L.; Muthukumar, L.; Herzberg, O. *Biochemistry* **2007**, *46*, 6911−6920.
(7) Lokeshwar, V. B.; Schroeder, G. L.; Selzer, M. G.; Hautmann, S. H.; Posey, J. T.; Duncan, R. C.; Watson, R.; Rose, L.; Markowitz, S.; Soloway, M. S. *Cancer* **2002**, *95*, 61−72.
(8) Zhong, Y.; Meng, F. H.; Deng, C.; Zhong, Z. Y. *Biomacromolecules* **2014**, *15*, 1955−1969.
(9) Lokeshwar, V. B.; Estrella, V.; Lopez, L.; Kramer, M.; Gomez, P.; Soloway, M. S.; Lokeshwar, B. L. *Cancer Res.* **2006**, *66*, 11219−11227.
(10) Roberts, J. J.; Elder, R. M.; Jayaraman, A.; Bryant, S. J. *Biomacromolecules* **2014**, *15*, 1132−1141.
(11) Eissa, S.; Kassim, S. K.; Labib, R. A.; El-Khouly, I. M.; Ghaffer, T. M.; Sadek, M.; Razek, O. A.; El-Ahmady, O. *Cancer* **2005**, *103*, 1356−1362.
(12) Thompson, C. B.; Shepard, H. M.; O'Connor, P. M.; Kadhim, S.; Jiang, P.; Osgood, R. J.; Bookbinder, L. H.; Li, X. M.; Sugarman, B. J.; Connor, R. J.; Nadjsombati, S.; Frost, G. I. *Mol. Cancer Ther.* **2010**, *9*, 3052−3064.
(13) Fennouri, A.; Przybylski, C.; Auvray, L.; Daniel, R. *ACS Nano* **2012**, *6*, 9672−9678.
(14) Yoffou, P. H.; Edjekouane, L.; Meunier, L.; Tremblay, A.; Provencher, D. M.; Mes-Masson, A.; Carmona, E. *PLoS One* **2011**, *6*, 1−12.
(15) Lee, H.; Lee, K.; Kim, I. K.; Park, T. G. *Biomaterials* **2008**, *29*, 4709−4718.

(16) Nossier, A. I.; Eissa, S.; Ismail, M. F.; Hamdy, M. A.; Azzazy, H. M. E. *Biosens. Bioelectron.* **2014**, *54*, 7−14.
(17) Chib, R.; Raut, S.; Fudala, R.; Chang, A.; Mummert, M.; Rich, R.; Gryczynski, Z.; Gryczynski, I. *Curr. Pharm. Biotechnol.* **2013**, *14*, 470−474.
(18) Du, J. J.; Hu, M. M.; Fan, J. L.; Peng, X. J. *Chem. Soc. Rev.* **2012**, *41*, 4511−4535.
(19) Chan, J.; Dodani1, S. C.; Chang, C. J. *Nat. Chem.* **2012**, *4*, 973−984.
(20) Carter, K. P.; Young, A. M.; Palme, A. E. *Chem. Rev.* **2014**, *114*, 4564−4601.
(21) Bacinello, D.; Garanger, E.; Taton, D.; Tam, K. C.; Lecommandoux, S. *Biomacromolecules* **2014**, *15*, 1882−1888.
(22) Mok, H. M.; Jeong, H. Y.; Kim, S. J.; Chung, B. H. *Chem. Commun.* **2012**, *48*, 8628−8630.
(23) Hu, J. M.; Zhang, G. Q.; Liu, S. Y. *Chem. Soc. Rev.* **2012**, *41*, 5933−5949.
(24) Li, K.; Liu, B. *Chem. Soc. Rev.* **2014**, DOI: 10.1039/C4CS00014E.
(25) Wang, X. D.; Wolfbeis, O. S. *Chem. Soc. Rev.* **2014**, *43*, 3666−3761.
(26) Yu, C. M.; Wu, Y. L.; Zeng, F.; Li, X. Z.; Shi, J. B.; Wu, S. Z. *Biomacromolecules* **2013**, *14*, 4507−4514.
(27) Guo, Z. Q.; Park, S.; Yoon, J. Y.; Shin, I. *Chem. Soc. Rev.* **2014**, *43*, 16−29.
(28) Deng, Y. H.; Feng, X. J.; Zhou, M. S.; Qian, Y.; Yu, H. F.; Qiu, X. Q. *Biomacromolecules* **2011**, *12*, 1116−1125.
(29) Yin, C. X.; Huo, F. J.; Zhang, J. J.; Martinez-Manez, R.; Yang, Y. T.; Lv, H. G.; Li, S. D. *Chem. Soc. Rev.* **2013**, *42*, 6032−6059.
(30) Santos-Figueroa, L. E.; Moragues, M. E.; Climent, E.; Agostini, A.; Martinez-Manez, R.; Sancenon, F. *Chem. Soc. Rev.* **2013**, *42*, 3489−3613.
(31) Lee, M. H.; Yang, Z. G.; Lim, C. W.; Lee, Y. H.; Sun, D. B.; Kim, J. S. *Chem. Rev.* **2013**, *113*, 5071−5109.
(32) Attar, H. A. Al.; Monkman, A. P. *Biomacromolecules* **2009**, *10*, 1077−1083.
(33) Yuan, L.; Lin, W. Y.; Zheng, K. B.; Zhu, S. S. *Acc. Chem. Res.* **2013**, *46*, 1462−1473.
(34) Wang, X.; Meier, R. J.; Wolfbeis, O. S. *Chem. Soc. Rev.* **2013**, *42*, 7834−7869.
(35) Wu, F.; Minteer, S. D. *Biomacromolecules* **2013**, *14*, 2739−2749.
(36) Li, X. H.; Gao, X. H.; Shi, W.; Ma, H. M. *Chem. Rev.* **2014**, *114*, 590−659.
(37) Feng, X. L.; Liu, L. B.; Wang, S.; Zhu, D. B. *Chem. Soc. Rev.* **2010**, *39*, 2411−2419.
(38) Jiang, B. P.; Guo, D. S.; Liu, Y. C.; Wang, K. P.; Liu, Y. *ACS Nano* **2014**, *8*, 1609−1618.
(39) Zhang, G. Q.; Yang, G. Q.; Wang, S. Q.; Chen, Q. Q.; Ma, J. S. *Chem.—Eur. J.* **2007**, *13*, 3630−3635.
(40) An, B. K.; Kwon, S. K.; Jung, S. D.; Park, S. Y. *J. Am. Chem. Soc.* **2002**, *124*, 14410−14415.
(41) Luo, J. D.; Xie, Z. L.; Lam, J W. Y.; Cheng, L.; Qiu, C. F.; Kwok, H. S.; Zhan, X. W.; Liu, Y. P.; Zhu, D. B.; Tang, B. Z. *Chem. Commun.* **2001**, 1740−1741.
(42) Hong, Y. N.; Lam, J. W. Y.; Tang, B. Z. *Chem. Soc. Rev.* **2011**, *40*, 5361−5388.
(43) Hong, Y. N.; Lam, J. W. Y.; Tang, B. Z. *Chem. Commun.* **2009**, 4332−4353.
(44) Ding, D.; Li, K.; Liu, B.; Tang, B. Z. *Acc. Chem. Res.* **2013**, *46*, 2441−2453.
(45) Zhao, Z. J.; Lam, J. W. Y.; Tang, B. Z. *Curr. Org. Chem.* **2010**, *14*, 2109−2132.
(46) Xie, H. F.; Zeng, F.; Yu, C. M.; Wu, S. Z. *Polym. Chem.* **2013**, *4*, 5416−5424.
(47) Gu, X. G.; Zhang, G. X.; Zhang, D. Q. *Analyst* **2012**, *137*, 365−369.
(48) Marei, W. F. A.; Salavati, M.; Fouladi-Nashta, A. A. *Mol. Hum. Reprod.* **2013**, *19*, 590−599.
(49) Stern, R. *Semin. Cancer Biol.* **2008**, *18*, 275−280.
(50) Choh, S. Y.; Cross, D.; Wang, C. *Biomacromolecules* **2011**, *12*, 1126−1136.
(51) Takahashi, T.; Ikegami-Kawai, M.; Okuda, R.; Suzuki, K. *Anal. Biochem.* **2003**, *322*, 257−263.